

Measurement of Characteristics of Sound Reflection and Scattering by Elastic Cylindrical Shells in Conditions of Hydroacoustic Basin

A. Kleshchev*

St. Petersburg State Marine Technical University, St. Petersburg, Russia

*Corresponding author: alexalex-2@yandex.ru

Received January 30, 2013; Revised March 04, 2013; Accepted March 10, 2013

Abstract A method and experimental setup intended for measurement the amplitude and phase of acoustic field in the near zone a scatterer are described. The results of measurement the scattering characteristics of low-frequency sound signals scattered by elastic cylindrical shells are analyzed.

Keywords: diffraction, Fresnel zone, Fraunhofer zone, Cylindrical shell, boundary conditions

1. Introduction

The following two problems are solved on the basis of experimental data on the amplitude - phase characteristics of the scattered sound field in the near zone of a scatterer made in the form of an elastic finite cylindrical shell [1,2]:

- 1). determination of the nature of sound scattering by the shell at low sounding frequencies;
- 2). calculation of the angular scattering in the Fraunhofer zone from the results of measurement the amplitude and phase of the scattered field in the Fresnel zone

2. The Criteria of the Acoustical Diffracted Measurements

The measurement of the characteristics of the sound reflection and scattering very often conduct at the models with an use for these intentions of the hydroacoustic basins and the shallow ponds and the water areas [3,4]. A principal difference of the diffracted experiment (DE) in the conditions of the hydroacoustic basin (HB) and the shallow water area (SWA) along a comparison with the natural conditions of a deep sea consists in a presence of the reflective boundaries disposed near to the source and scatterer (a free surface, a bottom, the walls of the basin). As a rule, the experimenters are interested by the characteristics of the reflection of a Fraunhofer zone (of a distant field) correspond-ding an infinite medium in that from the infinitely removed source on the scatterer falls a sound plane wave.

Therefore by the DE in the conditions of the HB or of the SWA by the principal problem is an except of an influence of the reflective boundaries of the division of the mediums on the characteristics of the scatterer. The solution of the this problem is begun witch a choise of the

form of the sound signal. The optimum properties with this point of view has a pulse signal with a harmonic or frequency – modulated filling. An use of the signal of the such type permits distinguish at a time the useful reflected signal by the body on a background of the preventing reflections from the boundaries. Therefore we are sparing the principal attention in the future the signals of the pulse type.

A distance between the source of pulse signal and the scatterer we will choose so as the wave, falling on the body, at least in the limits of the scatterer, could be received for the plane wave (littely from it differed). A receiver (a hydrophone) of the reflected signal we will place in the Fraunhofer zone. The criterions of the minimum distance between the combined antenna and the scatterer answering the two brought demands and founded on a known formula $R_{\min} \gg D^2/\lambda$ (D is the maximum dimension of the scatterer, λ is the length of the sound wave in the medium) were considered in [3,5]. However in the diffracted measurements the criterion of the minimum distance can be found with the help of the radial wave functions being by the fundamental solutions of the of the scalar Helmholtz equation [6,7]. We are showing this on the example of the bodies of the simplest form (a sphere, an infinite cylinder, prolate and oblate spheroids) or the bodies round that can circumscribe the spherical, cylindrical or spheroidal surfaces. At first we are determining a difference in the angular characteristics of the scattering by these bodies of the plane and spherical sound waves (for the cylinder we will conduct the comparison between the plane and cylindrical waves). For this we are write the decomposition of a potential of the spherical (or cylindrical) wave in series at the own functions of the Helmholtz equation [8]:

- 1). in the spherical coordinate system

$$\exp(ikR)/R = ik \sum_{n=0}^{\infty} (2n+1) P_n(\cos\theta) j_n^{(i)}(kr_1), \quad r_1 > r > 0, \quad (1)$$

where R - the distance between the source and the point of an observation; r - the radial coordinate of the point of an observation; r_1 - the radial coordinate of the source; θ - the angular coordinate of the point of the observation relatively of a polar axis;

2). in the circular cylindrical coordinate system

$$H_0^{(1)}(kR) = \sum_{n=0}^{\infty} \varepsilon_n J_n(kr) H_n^{(1)}(kr_1) \cos n\varphi, \quad r_1 > r > 0, \quad (2)$$

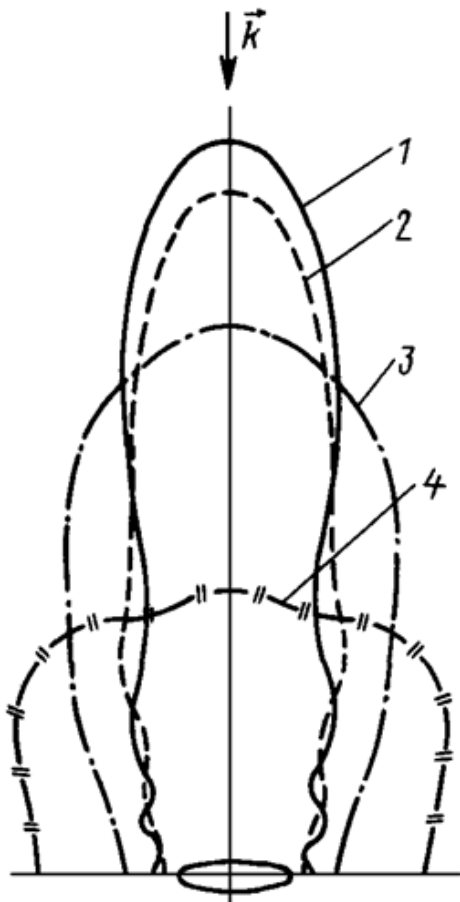
where r_1 , r and R form a triangle by that the angle φ is concluded between sides r and r_1 ;

$$\varepsilon_n = \begin{cases} 1 & \text{by } n = 0; \\ 2 & \text{by } n \neq 0; \end{cases}$$

3). in the prolate spheroidal coordinate system

$$\exp(ikR)/R = 2ik \sum_{m=0}^{\infty} \sum_{n \geq m}^{\infty} \varepsilon_m \bar{S}_{m,n}(C, \eta_1) \bar{S}_{m,n}(C, \eta') \times R_{m,n}^{(3)}(C, \xi_1) R_{m,n}^{(1)}(C, \xi') \cos m\phi, \quad \xi_1 > \xi', \quad (3)$$

where $\xi_1, \eta_1 (\eta_1 = \cos \theta_1), \phi_1 = 0$ - the spheroidal coordinates of the source; $\xi', \eta' (\eta' = \cos \theta')$, ϕ - the spheroidal coordinates of the point of the observation.



1 - the plane wave ; 2 - $\xi_1 = 10$;
3 - $\xi_1 = 2, 4$; 4 - $\xi_1 = 1, 1$

Figure 1. The moduluses of the angular characteristics of the soft spheroid

Analogously (3) will look the decomposition of the potential of the spherical wave and in the oblate

spheroidal coordinate system, only C must substitute on $-iC$, ξ_1 on $i\xi_1$ and ξ' on $i\xi'$. So in future we are limited by the prolate spheroidal coordinate system, remembered what we can cross to the oblate coordinates by a simple substitution of the wave dimension and the radial coordinate.

The formulas for the potential of the plane wave are got from (1) - (3), if r_1 and ξ_1 direct to the infinite and instead of the radial functions of third type and the Hankel functions use by their asymptotical meanings [2,6]. We are writing these asymptotics for the radial functions in the chosen us coordinate systems [2,6]:

1). in the spherical coordinate system

$$h_n^{(1)}(kr_1) \underset{kr_1 \rightarrow \infty}{\cong} (1/kr_1) i^{1-n} \exp(ikr_1); \quad (4)$$

2). in the cylindrical coordinate system

$$H_n^{(1)}(kr_1) \underset{kr_1 \rightarrow \infty}{\cong} \sqrt{2/\pi kr_1} \exp[ikr_1 - i(\pi/2)(n+1/2)]; \quad (5)$$

3). in the prolate spheroidal coordinate system

$$R_{m,n}^{(3)}(C, \xi_1) \underset{C\xi_1 \rightarrow \infty}{\cong} (i^{-n-1}/C\xi_1) \exp(iC\xi_1). \quad (6)$$

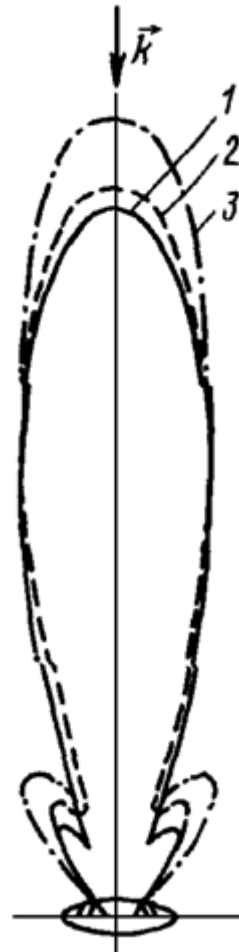


Figure 2. The moduluses of the characteristics of the sound scattering of the hard spheroid

In the real situations we have an affair with the terminal meanings r_1 and ξ_1 , however and in this case we can accomplish correctly a passage from the spherical (or cylindrical) wave to the plane wave (the field of the falling wave) or from the Fresnel zone in the Fraunhofer zone

(the field of scattered wave). We apply to the decompositions (1) - (3). The convergence of the series standing in the right parts of these formulas depends from this as quickly are diminished (over the modulus) with a growth of the indexes of the summing up the products of the radial functions of the first and third types. The number of the member of the series (n_{lim}, m_{lim}), on that must finish the summing up can be determined from the tables of the radial functions, it will by the function of the wave dimension kr_0 (the sphere, the cylinder) or C (the spheroid), of the coordinate r or ξ [in the given case it corresponds the coordinate of the external surface of the scatterer (r_0 or ξ_0) or circumscribed round it the the coordinate surface] and of the requisite precision. For a practical intention we can be limited by the members by that the modulus of the product of the radial functions of the first and third types at 3 - 4 order less of the biggest modulus of the product of these functions by the less meanings of the indexes. Now at the tables of the radial functions we are finding the limital meanings of the indexes of the summing up to that the and the sphere n_{lim} has the order kr_0 , by the spheroid n_{lim0} ($m=0$) of the order $C\xi_0$, by $m>0$ the meaning $n_{lim m}$ is diminished with the growth m , in other words $n_{lim m} \geq n_{lim m+1}$ has one and the same order what and $C\xi_0/2$. We are showing an use of the given method of the choice of the position of the point source relatively of the scatterer on example of the prolate spheroid with the coordinate of the external surface $\xi_0=1,005$, the wave dimension of the body C we are placing equal $10,0$. The angular coordinates of the source will invariable ($\theta_0=90^\circ, \varphi_0=0^\circ$), but the it radial coordinate ξ_l are giving two meanings $\xi_l'' = 2,4; \xi_l''' = 10,0$. From the tables of the radial functions we are putting, what the functions of the third type $R_{m,n}^{(3)}(10; \xi_l)$ must answer to the asymptotic (6) at least by the following meanings of the indexes: $m=0; n=0; 1; 2; 3; \dots; 13; m=1; n=1; 2; \dots; 13; m=2; n=2; 3; \dots; 12; m=3; n=3; 4; \dots; 11; m=4; n=4; 5; \dots; 10; m=5; n=5; 6; 7; 8$. In the tables 1 and 2 are presented the tabulated and asymptotical [from (6)] meanings of the radial functions of the third type with the indexes $m=0; n=0-13$ and the radial coordinate $\xi_l = 2,4$;

$10,0$. The difference between the tabulated and asymptotical meanings of the functions of the third type by $\xi_l = 2,4$ leads to the difference of the angular characteristics of the backscattering of the soundsoft spheroid of the wave from the point source with these radial coordinates, over the comparison with the angular characteristics of the scattering of the plane falling wave (Figure 1). As well can be placed the boundary of the Fraunhofer zone for the ideal scatterers in the form of the sphere, the cylinder or the spheroid (or near to them forms). However in this case the numbers of the indexes n_{lim} (the sphere, the cylinder) or n_{lim} and m_{lim} (the spheroid) of the radial functions of the third type for that must be fulfilled the asymptotical formulas (4) - (6) are determined more complicated combination of the radial functions of the first and third types (by the hard scatterer appear and the derivatives of these functions), entering in the coefficients of the decomposition of the pressure in the scattered wave over the own functions of the Helmholtz equation. The concrete formula for these coefficients is settled proceeded from the form of the boundary conditions and the type of the source of the falling on the body wave. For the ideal scatterer in the form of the prolate spheroid the combination of the radial functions has the following form:

the point source

a) the soft spheroid

$$R_{m,n}^{(3)}(C, \xi_l) R_{m,n}^{(3)}(C, \xi) R_{m,n}^{(1)}(C, \xi_0) / R_{m,n}^{(3)}(C, \xi_0); \quad (7)$$

b) the hard spheroid

$$R_{m,n}^{(3)}(C, \xi_l) R_{m,n}^{(3)}(C, \xi) R_{m,n}^{(1)'}(C, \xi_0) / R_{m,n}^{(3)'}(C, \xi_0); \quad (8)$$

the plane wave

a) the soft spheroid

$$R_{m,n}^{(3)}(C, \xi_l) R_{m,n}^{(1)}(C, \xi_0) / R_{m,n}^{(3)}(C, \xi_0); \quad (9)$$

b) the hard spheroid

$$R_{m,n}^{(3)}(C, \xi) R_{m,n}^{(1)'}(C, \xi_0) / R_{m,n}^{(3)'}(C, \xi_0). \quad (10)$$

Table 1. The radial spheroidal functions

$\xi_l = 2,4; C = 10,0; R_{m,n}^{(3)} = R_{m,n}^{(3)} \cdot 10^p$							
m	n	$R_{m,n}^{(3)}$	P	φ_n	$R_{m,n}^{(3)}$	P	φ_n
0	0	0,483 791	-1	1,59609	0,416 667	-1	3,57965
0	1	0,442 519	-1	0,43352	0,416 667	-1	2,00885
0	2	0,446 166	-1	5,53100	0,416 667	-1	0,43806
0	3	0,449 671	-1	4,31791	0,416 667	-1	5,15044
0	4	0,452 944	-1	3,07033	0,416 667	-1	3,57965
0	5	0,455 873	-1	1,78043	0,416 667	-1	2,00885
0	6	0,458 548	-1	0,45951	0,416 667	-1	0,43806
0	7	0,460 463	-1	5,43496	0,416 667	-1	5,15044
0	8	0,465 780	-1	4,18021	0,416 667	-1	3,57965
0	9	0,469 452	-1	2,98669	0,416 667	-1	2,00885
0	10	0,474 786	-1	1,84981	0,416 667	-1	0,43806
0	11	0,481 095	-1	0,76687	0,416 667	-1	5,15044
0	12	0,488 562	-1	6,02037	0,416 667	-1	3,57965
0	13	0,497 836	-1	5,04449	0,416 667	-1	2,00885

Table 2. The radial spheroidal functions

$\xi_l = 10; C = 10,0; R_{m,n}^{(3)} = R_{m,n}^{(3)} \cdot 10^p$							
m	n	$R_{m,n}^{(3)}$	p	φ_n	$R_{m,n}^{(3)}$	p	φ_n
0	0	0,985 006	-2	3,69860	0,100 000	-1	4,18142
0	1	0,102 257	-1	2,23514	0,100 000	-1	2,61062
0	2	0,984 224	-2	0,74773	0,100 000	-1	1,03983
0	3	0,102 381	-1	5,54127	0,100 000	-1	5,75222
0	4	0,985 668	-2	4,05154	0,100 000	-1	4,18142
0	5	0,102 319	-1	2,53228	0,100 000	-1	2,61062
0	6	0,988 064	-2	1,03498	0,100 000	-1	1,03983
0	7	0,102 162	-1	5,78615	0,100 000	-1	5,75222
0	8	0,991 795	-2	4,31125	0,100 000	-1	4,18142
0	9	0,100 615	-1	2,83078	0,100 000	-1	2,61062
0	10	0,100 665	-1	1,35651	0,100 000	-1	1,03983
0	11	0,100 719	-1	6,17562	0,100 000	-1	5,75222
0	12	0,100 780	-1	4,72436	0,100 000	-1	4,18142
0	13	0,100 846	-1	3,28267	0,100 000	-1	2,61062

If used by the formulas (9) and (10), we are finding the boundary ξ of the Fresnel zone and Fraunhofer zone of the scattered pressure for the plane falling wave and place on this boundary the point source ($\xi_l = \xi$), that as is seen from the comparison (7) and (8) with (9) and (10), this boundary will general for both types indignation. In a confirmation of this in Figure 2 come up the angular characteristics of the sound scattering by the hard spheroid of the pressure in the Fraunhofer zone for the plane and spherical waves. In Figure 2 the curve 1 corresponds the modulus of the angular characteristic of the sound scattering by the hard spheroid for the plane falling wave; the curve 2 corresponds the point source with the coordinate $\xi_l = 10,0$ and the distribution of the modulus of the scattered pressure for the radial coordinate $\xi_l = 10,0$ by the falling plane wave*; the curve 3 characterises the distribution of the modulus of the scattered pressure for the radial coordinate $\xi_l = 10,0$ (it is by the coordinate of the source).

The fulfilled numerical estimations shown, what the minimal distance R_{min} from the scatterer to the boundaries of the Fresnel and Fraunhofer zones submits to an inequality $R_{min} \geq 2(D^2/\lambda)$.

We see, what for the scatterers of the spheroidal form the linear distance from the surface of the scatterer ξ_0 until a line of the boundary ξ_2 depends from the angle of the observation θ : by biggest it will for the angle $\theta = 0^\circ$ and by least for the angle $\theta = 90^\circ$ (the oblate spheroid, for the prolate spheroid— backwards: maximum by $\theta = 90^\circ$; minimum by $\theta = 0^\circ$).

We are noticing as well, what by the angle $\theta = 0^\circ$ (the axially symmetric problem), the index m in the all higher written formulas has one meaning $m = 0$.

By the diffracted measurements in the natural ponds must remember about the following principal demands that they must answer [3]: 1) have enough the big dimensions so as an interference evoked by the reflections from the way of an use of the pulse regime; 2) posses by a low level of a surrounded noise; 3) the liquid medium must be free from all, what can evoke the refraction or the scattering of the sound (of the flows, of the gradients of

the temperaturature, of the sea organisms, of the bubbles and of the soilings).

For a securing of the low level of the surrounded noise, of a stability of a platform and of the conveniences of a production of the measurements must be fulfilled a protection from rainy weather.

By the source of the noise are the ships, disposed near from the basin, the industrial plants (especially the connected with a water pumps), a freight transport, the railroads, a rain, and the waves.

The auxiliary platforms, using by the measurements, are different: the piers, the bridges, the barges, but as well the ships. The piers and the bridges secure the best conveniences and the stability of the conditions of a work. If the basin is big and deep must use a sailing construction, but the stability and the conveniences must secure by a vertical dimension of the construction and by the service lines going under the water or coming to a shore.

Of the simple criterion for a definition of the minimal acceptable depth by the production of the measurements in the basin is not, but the requisite depth in a first turn is determined by the frequency range of the reflective body.

A quality of the hydroacoustic basin depends from that in which degree can remove an influence of the reflections or of the hindrance from the reflections. If the reflections are abolished or absorbed by the absorbes an the boundaries of the basin then last is named by drowned.

The big part of the such hydroacoustic basins are not above and they are similar the natural basins, but less them at the dimensions. By an exeption is the reserved drowned basin, in that can imitate the conditions of the measurements of the deep ocean given the high static pressures and the low temperature of the water.

By the pulse regime of the work the form of the basin is not important. By a limiting factor is the distance until reflective boundaries surfaces nearest to the way of the propagation of the straight acoustic signal from a source to ta scatterer and to a receiver.

3. The Structure Schema of the Experiment and it Methodology

The block diagram of the plant for the amplitude - phase measurements of the reflected (scattered) signal is presented in Figure 3. The block diagram includes in itself the radiating section, the scatterer (model) and the liquid

* The distribution of the scattered by the body pressure of the plane wave along the surface ξ_l in the conormity with the theorem of the mutuality coincides with the angular characteristic of the of the scattering of the wave from the point source, finding on this surface.

medium. We explain the principle its work, used the time diagrams of voltages in the radiating section (Figure 4). The generator of the harmonic oscillations G creates the harmonic signal of the frequency ω (see the diagram I on the Figure 4), the frequency that is controlled by the crystal - controlled digital frequency meter Fr. Entered on the modulator Mod, creating the rectangular video pulse by the duration τ (see the diagram II in Figure 4), the harmonic signal is turned in the pulse signal with the rectangular envelope and the harmonic filling of the frequency ω (see the diagram III in the Figure 4). This pulse signal with the help of the source S exposes to the sound the liquid medium of the the basin or of the water area and the finding in it model M. The hydrophone H (the receiver in Figure 3) can receive the different signals (in the dependence from the situation). If turns out well divide the useful signal p_s (reflected from the model) and the hindrance p_p (the reflection from the boundaries of the division of the mediums), then the receiver fixes the signal p_s , scattered of the model. If the model is absent, then the hydrophone receives only the straight signal p_i . If the receiver is disposed near of the model, then the division of the straight and scattered signals can not and the hydrophone fixes the diffracted pulse signal.

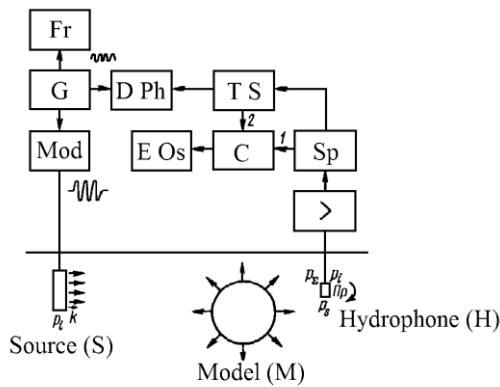


Figure 3. The block diagram of the plant for the measurement of the sound scattering

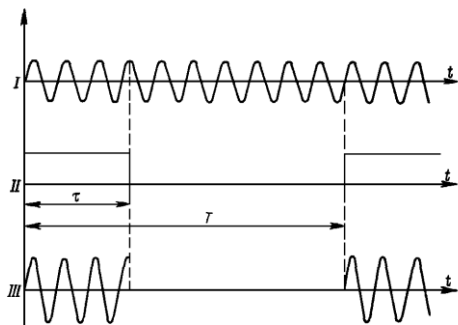


Figure 4. The time diagrams of the voltages in the radiating section of the plant

At the low frequencies, interfering reflections can be avoided only near the model. In this case, it is almost impossible to separate the direct and reflected signals and the measurement receiver detects the total (diffracted) signal. If the undistorted signal (obtained without the

model) is known at the same points, the scattered signal can be determined as the difference between the diffracted and straight signals (under the condition that the amplitudes and phases of these signals are measured simultaneously). From the distributions of the scattered or diffracted signals, measured near the model, it is possible to calculate the angular characteristics (the characteristics of the far field of the scatterer) by using the Kirchoff integral [7,9,10]. In acoustics, the method of extrapolating the near - field data to the far field was first applied to hydroacoustics arrays (in the literature, this method has been called the DRL method) [3,5,8,11]).

The sound pulse (p_s, p_i or p_Σ), turned by the hydrophone in electric signal, dos at the preliminary amplifier $>$, but after at the spectrometer Sp of the ultrasonics frequencies, tuned in the frequency of the filling of the pulse ω . Further the signal follows over the two channels: over the first channel the signal filtered out by the spectrometer Sp is given at the time selector TS that, cuts out 1 - 2 the periods of the placing part of the pulse. The pulse signal with the time selector and the harmonic signal with the generator G of the harmonic oscillations do at the two entrances of the digital phase - meter DPh, that measures the phase of the signal, receiving by the hydrophone, relatively of the supportal signal with the generator G. поступают Simultaneously the signal with the spectrometer Sp dos at the first entrance of the commutator C, at it the second entrance dos the signal with the time selector TS and in the dependence from the position of the relay of the commutator on the screen of the cathode - ray oscilloscope EOs we observe either the all time picture of the pulses in the liquid medium (in the time of the time - base) or the placing part of the useful signal cut out by the time selector TS.

We are telling about the method DRL on the example of the diffracted problem [7,9]. If we know the distribution of the scattered p_s or diffracted $p_\Sigma = p_i + p_s$ pressures on the surface S, surrounding the scatterer, then with the help of the Kirchoff integral we can determine $p_s(P)$ or $p_\Sigma(P)$ in the any arbitrary point of the observation P [1,2,3,5,7,9,10]:

$$p_s(P) = (1/4\pi) \iint_S \left\{ \left[\frac{\partial p_d(Q)}{\partial n} \right] G(P; Q) - p_d(Q) \left[\frac{\partial G(P; Q)}{\partial n} \right] \right\} dS \quad (11)$$

where: the index d is s or Σ , Q - the point of the surface S; $G(P; Q)$ - the Green function, submitting to the non - homogeneous Helmholtz equation [2].

Chosen $G(P; Q)$ such, what on the surface S it itself disappears G_1 or turns into zero its normal derivative G_2 , we are getting the two other integral formulas*:

$$p_s(P) = -(1/4\pi) \iint_S p_d(Q) \left[\frac{\partial G_1(P; Q)}{\partial n} \right] dS; \quad (12)$$

$$p_s(P) = (1/4\pi) \iint_S \left[\frac{\partial p_d(Q)}{\partial n} \right] G_2(P; Q) dS. \quad (13)$$

* By writing down (11) - (13) took into account, what the Kirchoff integral for the pressure p_i in the falling wave equally zero [12].

For the surfaces S of the spheroidal or spherical forms the formulas for G_1 and G_2 have according the following form [2]:

$$G_1(\xi, \eta, \phi; \xi', \eta', \phi') = 2ik \sum_{n=0}^{\infty} \sum_{m=-n}^n \bar{S}_{m,n}(C, \eta) \bar{S}_{m,n}(C, \eta') \times \exp[im(\phi - \phi')] \left[R_{m,n}^{(1)}(C, \xi') R_{m,n}^{(1)}(C, \xi) - R_{m,n}^{(3)}(C, \xi') R_{m,n}^{(3)}(C, \xi) \right] \times R_{m,n}^{(1)}(C, \xi_0) R_{m,n}^{(3)}(C, \xi') / R_{m,n}^{(3)}(C, \xi_0), \quad \xi > \xi'; \quad (14)$$

$$G_2(\xi, \eta, \phi; \xi', \eta', \phi') = 2ik \sum_{n=0}^{\infty} \sum_{m=-n}^n \bar{S}_{m,n}(C, \eta) \bar{S}_{m,n}(C, \eta') \times \exp[im(\phi - \phi')] \left[R_{m,n}^{(1)}(C, \xi') R_{m,n}^{(3)}(C, \xi) - R_{m,n}^{(3)}(C, \xi') R_{m,n}^{(1)}(C, \xi_0) \right] \times R_{m,n}^{(3)}(C, \xi') / R_{m,n}^{(3)}(C, \xi_0), \quad \xi > \xi'; \quad (15)$$

$$G_1(r, \theta, \phi, r', \theta', \phi') = ik \sum_{n=0}^{\infty} (2n+1) \sum_{m=-n}^n \left[(n-m)! / (n+m)! \right] \times P_n^m(\cos \theta) P_n^m(\cos \theta') \exp[im(\phi - \phi')] \left[j_n(kr') h_n^{(1)}(kr) - j_n(kr_0) h_n^{(1)}(kr) h_n^{(1)}(kr') / h_n^{(1)}(kr_0) \right], \quad r > r'; \quad (16)$$

$$G_2(r, \theta, \phi, r', \theta', \phi') = ik \sum_{n=0}^{\infty} (2n+1) \sum_{m=-n}^n \left[(n-m)! / (n+m)! \right] \times P_n^m(\cos \theta) P_n^m(\cos \theta') \exp[im(\phi - \phi')] \left[j_n(kr') h_n^{(1)}(kr) - j_n'(kr_0) h_n^{(1)}(kr) h_n^{(1)}(kr') / h_n^{(1)}(kr_0) \right], \quad r > r'; \quad (17)$$

where $\xi, \eta, \phi; r, \theta, \phi$ – the spheroidal and spherical coordinates of the point of the observation P ; $\xi', \eta', \phi'; r', \theta', \phi'$ – the spheroidal and spherical coordinates of the point Q of the surface S ; in the given case $\xi = \xi_0$ and $r' = r_0$.

An advantage of the termal integrals (12) and (13) at the comparison with the binominal (11) obviously: for the definition of the pressure in the distant field enough know the distribution only of the pressure $p_d(Q)$ or only its normal derivative $dp_d(Q)/dn$ along the surface S . The formulas (14)–(17) get simplified [13] for the account of the substitution of the radial functions $R_{m,n}^{(3)}(C, \xi)$ and $h_n^{(1)}(kr)$ their asymptotical meanings, what is fairly for the distant field (for the Fraunhofer zone).

By the use of the binominal integral (11) as the Green function $G(P; Q)$ we choose

$$G(P; Q) = \exp(ikr)/r, \quad (18)$$

where r – the distance between the points P и Q . Besides that, from the absence the enough miniature receivers of the oscillatory velocity use one from two approximation:

1) the scattered wave near of the surface S we account by plane and spreading normally to it, in the result the measurement of the normal derivative $dp_s(Q)/dn$ is become unnecessary as $dp_s(Q)/dn = ikp_s(Q)$;

2) the measurement of the derivative $dp_s(Q)/dn$ we substitute by the relation of the terminal differences of the pressures $[\Delta p_s(Q)]$ and the distances Δq between the surfaces of the measurements S_1 and S_2 :

$$dp_s(Q)/dn \approx \Delta p_s(Q) / \Delta q.$$

In the Fraunhofer zone (r is enough big) are fair the usual approximations [6]:

$$p_s(P) = D(\theta, \phi) \exp(ikR)/R, \quad (19)$$

where R – the distance from the beginning of the coordinates of the system O to the point of the observation; $D(\theta, \phi)$ – the angular characteristic of the scattering in the spherical coordinates θ, ϕ ;

$$\begin{aligned} (\partial/\partial n) [\exp(ikr)/r] &\approx (\partial/\partial n) [\exp(ikR)/R] \\ &\approx ikR^{-1} \exp(ikR) (\partial R/\partial n) = ikR^{-1} \cos \theta' \exp(ikR), \end{aligned} \quad (20)$$

In the distant zone the single vector from Q in P can substitute by the single vector \vec{m} from the point O in the point P , so what

$$\cos \theta' = m_x n_x + m_y n_y + m_z n_z.$$

On the practice the continuous distributions of the pressure $p_s(Q)$ and of the normal derivative $dp_s(Q)/dn$ are substituted by discrete and from the integrals we come to the numerical quadratures for the both approximations [1,2,7,9]

$$\begin{aligned} D(\theta, \phi) &= (ih_0 C / 4\pi) (\xi_0^2 - 1)^{1/2} \int_0^{2\pi} \int_{-1}^1 d\phi' [-p_d(Q) \cos \theta' + p_d(Q)] \\ &\times (\xi'^2 - \eta'^2)^{1/2} \exp(iB) d\eta' = (ih_0 C / 4\pi) (\xi_0^2 - 1)^{1/2} \sum_{m=1}^M D_m \sum_{l=1}^L A_l \\ &\times \Phi_1(\eta'_l, \phi'_m), \quad \xi' = \xi_0; \quad d = S \text{ or } \Sigma; \end{aligned} \quad (21)$$

$$\begin{aligned} D(\theta, \phi) &= (h_0^2 / 4\pi) (\xi_0^2 - 1)^{1/2} \int_0^{2\pi} \int_{-1}^1 d\phi' [-p_d(Q) ik \cos \theta' + [\Delta p_d(Q) / \Delta q]] \\ &\times (\xi'^2 - \eta'^2)^{1/2} \exp(iB) d\eta' = (h_0^2 / 4\pi) (\xi_0^2 - 1)^{1/2} \sum_{m=1}^M D_m \sum_{l=1}^L A_l \\ &\times \Phi_2(\eta'_l, \phi'_m), \quad \xi' = \xi_0; \quad d = S \text{ or } \Sigma; \end{aligned} \quad (22)$$

where $\Phi_1(\eta'_l, \phi'_m)$ and $\Phi_2(\eta'_l, \phi'_m)$ – the meanings of the corresponding integrand functions in the nodes of the numerical quadratures; L and M – the number of the nodes after the coordinates η' and ϕ' according; A_l and D_m – the main coefficients; the formulas for $\cos \theta'$ and B are given in [8]. By the use (22) for the calculation of the relation $\Delta p_d(Q) / \Delta q$ we measure the pressures on the two enough near disposed confocal surfaces (the distance between them much less of the length of the sound wave λ in the liquid). For the exception of the influence of the nonhomogeneous flexural waves (for the scatterers in the form of the elastic shells) the distance from the surface of the scatterer to the nearest (main) point must not be $\lambda/2$, the distance between the main points so as we could avoid of the false additional maximums must be less $\lambda/2$.

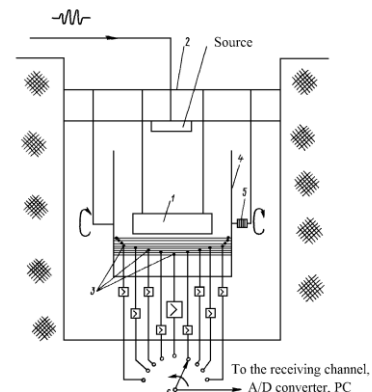


Figure 5. The angular gear for the measurements of the distributions in the near zone

The measurement of the distributions of the diffracted pressure near of the model can be fulfilled with the help of the construction, presented in Figure 5. The model 1 is suspended to the construction 2 with the help of the metallic strings. The miniature hydrophones 3 are fixed to the strings of angular gear 4 made from hollow (water-filled) metal tubes. For correct phase measurements, the hydrophone size should be small compared to the

wavelength of sound. The low-speed electric motor 5 served to rotate the angular gear around the model at the required step in angle. At each fixed position of the system, the amplitude - phase distribution of the diffracted pressure was measured with the use of switch 6 and the receiving channel of the experimental setup (see Figure 5). Through the A/D converter, the distribution was sent to the PC, where the angular characteristic was calculated.

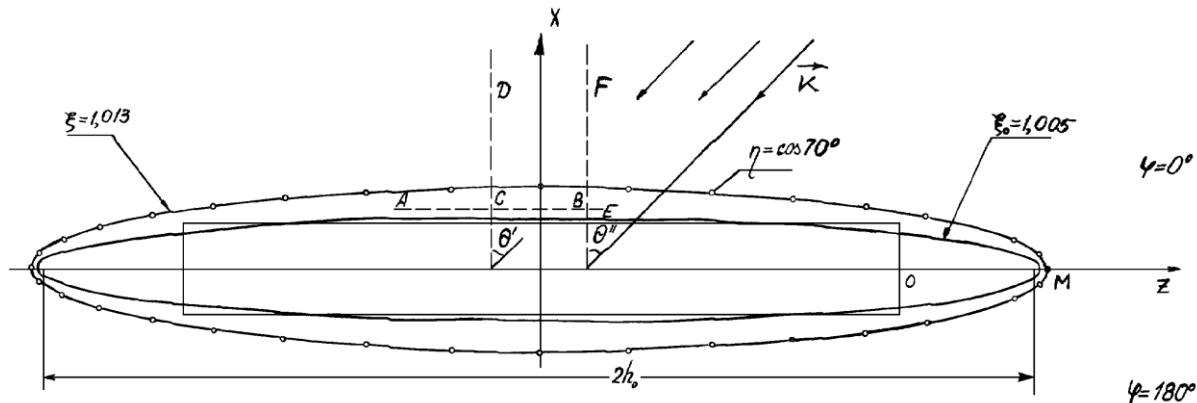


Figure 6. The measuring directions AB, CD, EF and OM; the measuring points; the contour of the cylindrical shell on the measuring template

The field, scattered by the elastic shell, was measured in the Fresnel zone by using the setup shown in Figure 5 and the structure shown in Figure 6. The latter consisted of the rigid template fixed above the water surface. The paper sheet was glued to the upper surface of the template. On the paper, the contour of a cylindrical shell with flat ends, the approximating contour of an elliptic shape, the measuring elliptic contour and the measurement lines AB, CD, EF and OM were drawn. Along the shell contour, the measuring elliptic contour and the AB, CD, EF and OM directions, holes served to suspend miniature spherical hydrophones with the diameter $d = 5\text{mm}$. The strings were strained with the use of a load, which was positioned near the bottom of the tank to eliminate its effect on the scattered sound field measurements [10].

In both types of the experimental setup, the angle at which the model was insonified could be varied by varying the position of the source with respect to the scatterer. The insonifying pulse length was always greater than the maximal size of the model.

As in the setup shown in Figure 1, the measurements were performed twice: first, in the presence of the shell, the magnitude of the diffracted pressure and its phase were measured, then the shell was lifted to the surface and the pressure magnitude and the phase of the incident wave were measured at the same points as before.

4. The Analysis of the Results of the Measurements

The measured amplitude – phase distributions of the diffracted or scattered field near the scattered allow determination of the factors that govern the scatterer field formation. Figure 7 shows the meanings of the magnitude and the phase of the scattered pressure for the finite cylindrical shell insonified along its rotation axis. At this axis (the OM direction in Figure 6), the distributions

of the magnitude and the phase were measured at different wave distances kz from the end of the shell with the radius a . Curves 1 and 2 represent the experimental values of the magnitude and the phase of the scattered pressure respectively. Curves 3 and 4 represent the corresponding distributions for the elastic hollow oblate spheroidal shell with the major semi-axis a in the case of its insonification along the OM direction [14]. Distributions 5 and 6 characterize the magnitude and the phase of the scattered pressure soft oblate spheroid, the wave size of the body $C = ka = 3,1$.

Figure 8 shows similar distributions of the magnitude and the phase of the scattered pressure for aforementioned spheroidal shell along the OM direction with another wave size $C = 1,0$.

Figure 9 and Figure 10 compare the experimental and calculated (for the acoustically soft infinite cylinder) distributions of the magnitude and the phase of the diffracted pressure, the distributions were measured along the EF direction, the data were obtained for bounded cylinders with the wave size $C = ka = 1,0$ (Figure 9) and $C = ka = 3,1$ (Figure 10). In addition, Figure 9 compares the distributions of the magnitude and phase of the diffracted pressure obtained for two shells (model 1 and model 2) with identical lengths and diameters but with different thicknesses of their ends. In both cases, the shells were insonified along the EF direction.

The structure represented in Figure 6 makes it possible (by recalculating the near field to the far field) to obtain the angular scattering characteristic $D(\theta)$ for axisymmetric models insonified along their rotation axis, because, in this case, it is not necessary to measure $|p_s|$ and ψ_s for different values of the angle φ . As the illustration, Figure 11 displays the results of the measurements the magnitude of the angular characteristic $|D(\theta)|$ for the aforementioned cylindrical shell with the use of the setup and method of measurement described above.

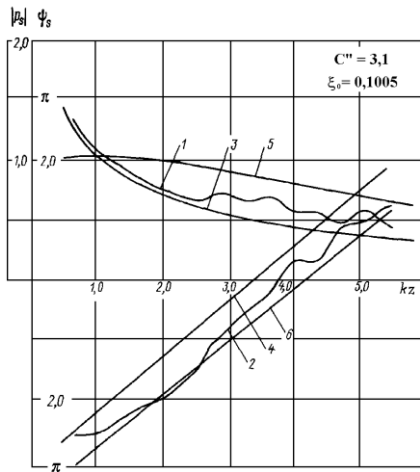


Figure 7. The magnitude – phase distributions of the scattered field

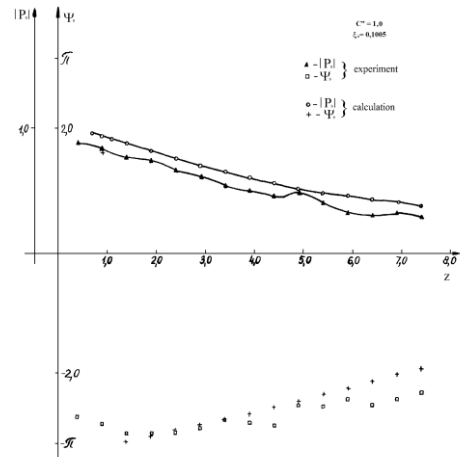


Figure 8. The calculated and experimental distributions of the magnitude and the phase of the scattered field

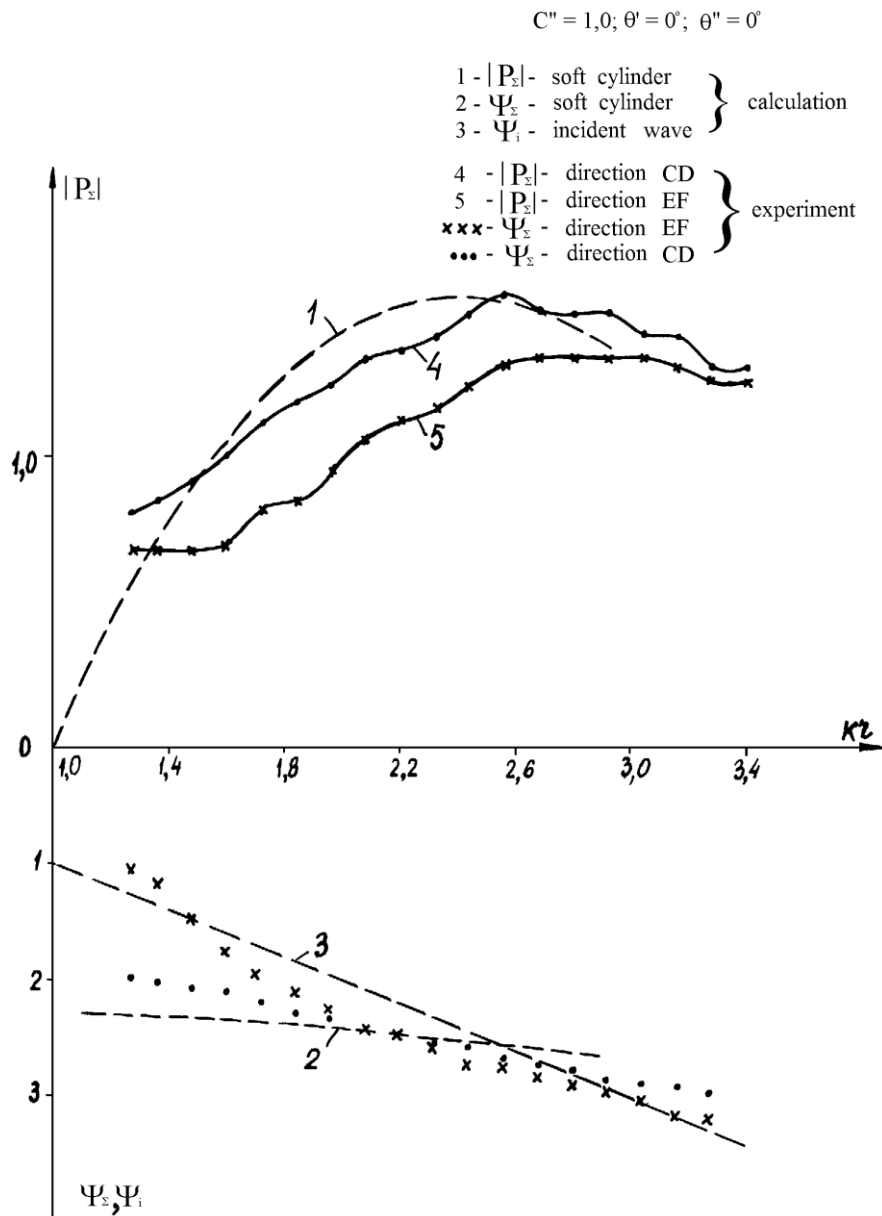


Figure 9. The calculated and experimental distributions of the magnitude and the phase of the diffracted field

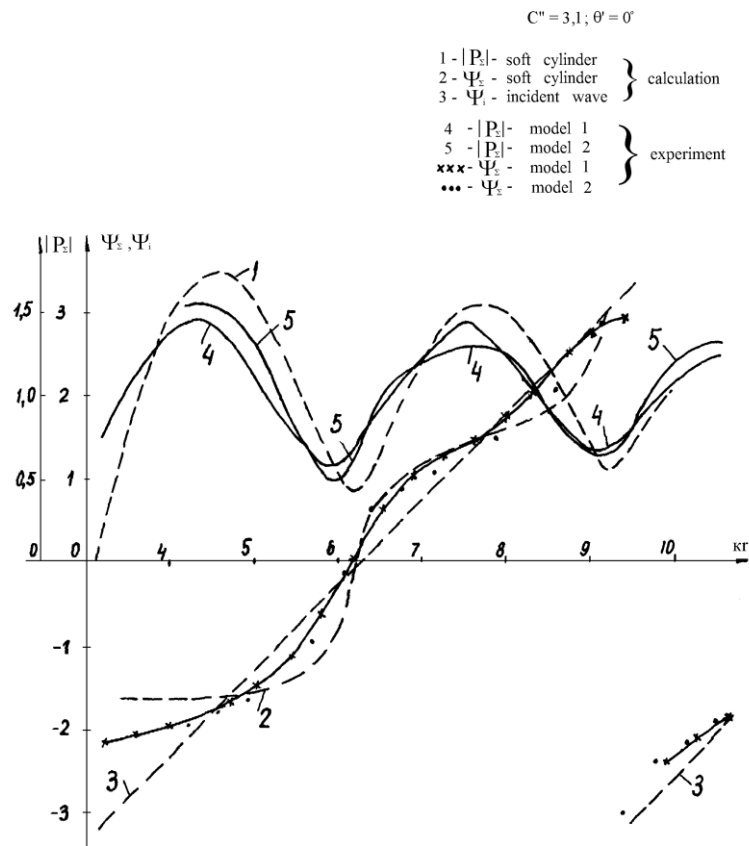


Figure 10. The calculated and experimental distributions of the magnitude and the phase of the diffracted field

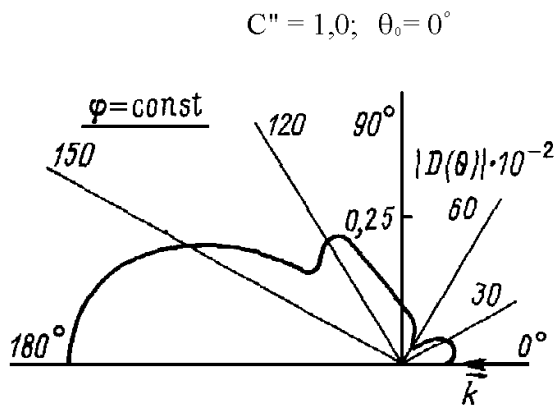


Figure 11. The modulus of the angular scattering characteristic of the hollow cylindrical shell

5. Conclusions

If the pulsed signal from the scatterer can be singled out in the Fraunhofer zone (the deep-water region), the angular scattering characteristic can be measured directly. However, this procedure is rather complicated, as compared to the method described above, because it requires scanning of the great number of points at the uniform step on the spherical surface in the far zone. In addition, it is necessary to select the useful scattered signal

against interfering reflections at all of the measurement points. Therefore, in experiments, as the rule, only two-dimensional (rather than three-dimensional) scattering characteristics are measured (or only parts of these characteristics).

Acknowledgments

The work was supported as of research under State Contract no P242 of April 21, 2010, within the Federal Target Program "Scientific and scientific - pedagogical personnel of innovative Russia for the years 2009 - 2013".

References

- [1] Kleshchev A. A., "Scattering of Low - Frequency Pulsed Sound Signals from Elastic Cylindrical Shells", *Acoust. Physics*. 57(3): 375-380, 2011.
- [2] Kleshchev A. A., *Hydroacoustic Scatterers*, Prima, St. Petersburg, 2012 [in Russian].
- [3] Bobber R., *Underwater Electroacoustic Measurements*, Peace, Moscow, 1974 [in Russian].
- [4] Klyukin I. I., Kolesnikov A. E., *Acoustic Measurements in Shipbuilding*, Shipbuilding, Leningrad, 1982 [in Russian].
- [5] Horton C. W., "Acoustic Impedance of an Outgoing Cylindrical Wave", *J. Acoust. Soc. Am.* 34 (10). 1663. Oct. 1962.
- [6] Kleshchev A. A., Klyukin I. I., *Principles of Hydroacoustics*, Shipbuilding, Leningrad, 1987 [in Russian].
- [7] Kleshchev A. A., Klyukin I. I., "The experimental method of the production of the characteristics of the far - field of the scatterers", *Tr. LKI*. 77: 37-40, 1972.

- [8] Horton C. W., Innis G. S., "The Comparison of Far - Field Radiation Patterns from Measurements Made Near the Source", *J. Acoust. Soc. Am.* 33(7): 877-880, 1961.
- [9] Kleshchev A. A., Klyukin I. I., "The use of the diffracted Kirchhoff integral for the calculation of the angular characteristics of scattering", in *7th All - Union Acoustic Conference*, Nauka, Leningrad, 123-125, 1973.
- [10] Kleshchev A. A., "The experimental characteristics of the scattering of the non - stationary sound signal by the cylindrical shells at the low frequencies in the Fresnel zone", in *21st Session of Russ. Acoust. Soc. Geos*, Moscow, 163-166, 2009.
- [11] Baker D. D., "Determination of Far - Field Characteristics of Large Underwater Sound Transducers from Near - Field Measurements", *J. Acoust. Soc. Am.* 34 (11): 1737-1744. Nov. 1962.
- [12] Shenderov E. L., *Wave Problems of Hydroacoustic, Shipbuilding*, Leningrad, 1982 [in Russian].
- [13] Kleshchev A. A., "The some criterions of the acoustical diffracted measurements", in *7th All - Union Acoustic Conference*. Nauka, Leningrad, 143-146, 1973.
- [14] Kleshchev A. A., "The scattering of the sound by the elastic oblate spheroidal shell", *Sov. Phys. Acoust.* 21 (6): 571-573, 1975.